Lipid Selectivity of the Calcium and Magnesium Ion Dependent Adenosinetriphosphatase, Studied with Fluorescence Quenching by a Brominated Phospholipid†

J. Malcolm East and A. G. Lee*

ABSTRACT: 1,2-Bis(9,10-dibromooleoyl)phosphatidylcholine (BRPC) has been prepared from dioleoylphosphatidylcholine (DOPC). It is shown that the gel to liquid-crystalline phase transition for BRPC occurs below ca. 5 °C and that the motional properties of bilayers of BRPC and DOPC as detected by spin-labeled fatty acids are similar. The ATPase activities of the (Ca^{2+}–Mg^{2+})-ATPase from rabbit muscle sarcoplasmic reticulum reconstituted with BRPC and DOPC are similar. The brominated lipid quenches the fluorescence of the ATPase and can be used to determine selectivity of lipid binding to the ATPase. We show that there is little selectivity on the basis of fatty acyl chain length. Binding constants for phosphatidylcholines and phosphatidylserines are similar in the absence of calcium, although that for phosphatidylserine decreases in the presence of calcium. Phosphatidylethanolamines bind less strongly than phosphatidylcholines, although the difference is small. The largest difference in binding constants is seen between phosphatidylcholines in the gel and liquid-crystalline phases, with a distribution coefficient of 30 in favor of the liquid-crystalline phase. It is shown that the distribution of the ATPase in mixtures of dipalmitoylphosphatidylcholine and BRPC can be understood in terms of the phase diagram for this mixture of lipids. Activities of the ATPase in the presence of mixtures of lipids can be explained in terms of the relative binding constants obtained from the fluorescence experiments.

One of the most successful approaches to the problem of membrane structure has been the reconstitution of a particular membrane function using defined and purified components. In this way it has been shown that the activity of a membrane protein such as the (Ca^{2+}–Mg^{2+})-ATPase[1] from sarcoplasmic reticulum of muscle depends on the chemical structure and physical state of the surrounding lipid. There is an optimal chain length for the lipid fatty acyl chains (Johannsson et al., 1981; Moore et al., 1981), and phosphatidylcholines support higher activities than other phospholipids (Bennett et al., 1978). In addition, protein activity is much greater when the surrounding lipid is in the liquid-crystalline phase than when it is in the gel phase (Warren et al., 1974a). In real membranes of course a wide variety of phospholipids are present and the question then arises as to whether proteins show different affinities for the different phospholipids present in the membrane, so that the lipid annulae around each protein will provide the protein with its own, appropriate, microenvironment. This is particularly important since the phospholipid composition of membranes changes with development, diet, and disease (Sarzala et al., 1973; Ansell et al., 1973).

In a recent paper, London & Feigenson (1981b) have shown how fluorescence quenching can be used to measure relative binding constants for lipids to the (Ca^{2+}–Mg^{2+})-ATPase without the necessity for macroscopic separations. They employed spin-labeled phospholipids as quenchers. In this paper we show that it is possible to perform similar experiments using the fluorescence quenching properties of lipids containing brominated fatty acyl chains and that have physical properties very similar to those of phospholipid containing unsaturated fatty acyl chains.

Molecules containing bromine are known to be efficient quenchers of the fluorescence of a wide variety of molecules, by a process referred to as heavy atom quenching and which involves an intimate collision between the fluorophor and the quencher (Parker, 1968; Berlman, 1973). A variety of ESR studies [see Hesketh et al. (1976); Knowles et al., 1981] have shown that exchange of phospholipids between the annulus around the ATPase and the bulk lipid is slow on the ESR time scale ($V_{ex} < 10^8$ s^{-1}). This can be compared to the fluorescence decay for the tryptophans of the (Ca^{2+}–Mg^{2+})-ATPase which is fast on the ESR time scale: although multiexponential, the fluorescence decay can be fitted to a sum of two exponentials with decay times of 1.9 and 4.9 ns with preexponential factors of 0.6 and 1.3, respectively (J. M. East, A. G. Lee, S. R. Meech, and D. Phillips, unpublished observations). Quenching of ATPase fluorescence by brominated phospholipids would therefore be expected to be a static process, caused by brominated phospholipids present in the annulus around the protein at the moment of excitation. Displacement of brominated phospholipids from the annulus by addition of a second, nonbrominated, phospholipid would reduce this quenching. The experiment can therefore readily give information about the relative affinities of phospholipids for the annular sites around the ATPase.

There are two advantages to the use of brominated phospholipids in these studies compared to the spin-labeled phospholipids previously employed. First, phospholipids with bromine-containing fatty acyl chains behave much like conventional phospholipids with unsaturated fatty acyl chains (see below). Second, the preparation of brominated phospholipids from the corresponding unsaturated phospholipids is trivial. The advantage of fluorescence techniques for studying lipid selectivity over ESR techniques employing spin-labeled phospholipids is one of scale. Because of the sensitivity of the

† From the Department of Biochemistry, University of Southampton, Southampton, S09 3TU, United Kingdom. *Received February 15, 1982.* Supported by the Science Research Council and the American Muscular Dystrophy Association.

[1] Abbreviations: BRPC, 1,2-bis(9,10-dibromooleoyl)-*sn*-glycero-3-phosphorylcholine; DOPC, 1,2-dioleoyl-*sn*-glycero-3-phosphorylcholine; DPPC, 1,2-dipalmitoyl-*sn*-glycero-3-phosphorylcholine; DMPC, 1,2-dimyristoyl-*sn*-glycero-3-phosphorylcholine; Tempo, 2,2,6,6-tetramethylpiperidinyl-1-oxy; ATPase, adenosinetriphosphatase; ESR, electron spin resonance; GLC, gas–liquid chromatography; TLC, thin-layer chromatography; Hepes, 4-(2-hydroxyethyl)piperazineethanesulfonic acid; EGTA, ethylene glycol bis(β-aminoethyl ether)-*N*,*N*,*N*′,*N*′-tetraacetic acid.

0006-2960/82/0421-4144$01.25/0

fluorescence technique, it is possible to employ the lipid-titration technique previously developed for determining effects of lipid on ATPase activity (Warren et al., 1974a). The technique involves simple incubation of ATPase and lipid in cholate solution followed by dilution into buffer for fluorescence determination, avoiding any time-consuming centrifugation steps.

Materials and Methods

Lipids were obtained from Sigma or Lipid Products and the fatty acid nitroxide probes and Tempo from Syva. The synthesis of 1,2-bis(9,10-dibromooleoyl)-*sn*-glycero-3-phosphorylcholine (BRPC) was as outlined in Dawidowicz & Rothman (1976). One hundred milligrams of dioleoylphosphatidylcholine (DOPC) in 5 mL of chloroform at −20 °C was reacted with 40 μL of bromine. The reaction was left for 30 min. Excess bromine was removed by adding the reaction mixture to a silicic acid column equilibrated with chloroform. The bromine was eluted with chloroform and 10% methanol–chloroform, and finally the BRPC was eluted with 50% methanol–chloroform. BRPC was stored in chloroform under nitrogen at −20 °C. Methyl esters of the fatty acid side chains, prepared by the method of Morrison & Smith (1964), were examined by GLC–mass spectrometry to confirm the identity of the compound, and purity was confirmed by TLC and by measuring bromine phosphorus ratios (Belcher & Nutten, 1960; Bartlett, 1959).

Phase transitions in BRPC/1,2-dipalmitoyl-*sn*-glycero-3-phosphorylcholine (DPPC) and DOPC/DPPC mixtures were measured by using the spin-label 2,2,6,6-tetramethylpiperidinyl-1-oxy (Tempo) after the method outlined by Shimshick & McConnell (1973). Lipid mixtures were prepared in chloroform, and 5.1 μmol was dried down to a thin film on the sides of a flask. One microliter of a 1 mg/mL solution of Tempo in chloroform was then added, followed by 20 μL of chloroform. After the mixtures were rotamixed, the chloroform was removed by nitrogen and 50 μL of buffer [Hepes (40 mM), NaCl (100 mM), and EGTA (1 mM), pH 7.2] added. The lipid suspension was sonicated for a few seconds, rotamixed, and heated to 45 °C until no lipid adhered to the walls of the flask. The sample was transferred to a glass capillary tube and the ESR spectrum run on a Bruker ER 200D spectrometer. The temperature of the sample was adjusted to around 278 K, and temperature scans were performed by increasing the temperature in 1–3 °C steps, allowing the sample to equilibrate for 2 min between steps.

The fluidities of BRPC and DOPC were characterized by using two spin-labeled fatty acid probes [*m*,*n*]SL

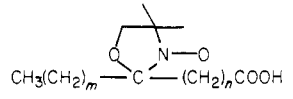

at a 100:1 lipid:probe molar ratio.

(Ca^{2+}–Mg^{2+})-ATPase was prepared from female rabbit (New Zealand White) hind leg muscle by a modification of the method of Warren et al. (1974b). Briefly this consisted of mincing about 500 g of muscle, followed by homogenizing the material in a blender for 2 min with 1.5 volumes of cold 0.3 M sucrose, 20 mM histidine, 1 mM dithiothreitol (DTT), and 5 μM phenylmethanesulfonyl fluoride (PMSF) (pH 8.0). The homogenate was centrifuged (8000*g*, 0 °C, 15 min). The undisrupted material was retreated as above, and the pooled supernatants were filtered through muslin and centrifuged (37000*g*, 90 min, 0 °C). The pellets were resuspended in 150 mL of cold 0.3 M sucrose, 10 mM histidine, 0.6 M KCl, 1 mM DTT, and 5 μM PMSF (pH 8.0) and left on ice for at least 30 min followed by centrifugation (37000*g*, 2 h, 0 °C). The pellet was resuspended in 3–5 mL of 0.25 M sucrose, 1 M KCl, and 50 mM potassium phosphate (pH 8.0). This buffer was used for all remaining procedures unless stated otherwise. This homogenate was dialyzed overnight against 1 L of buffer. Pure SR ATPase was isolated by treating the dialyzed fraction (protein concentration >30 mg/mL) with 100 mg/mL potassium cholate in buffer, to give 0.4 mg of cholate/mg of protein. This material was loaded onto a discontinuous sucrose gradient (20%/30%) with a 60% cushion, in 1 M KCl and 50 mM potassium phosphate (pH 8.0) and centrifuged overnight (95000*g*, 0 °C). The pure SR ATPase was collected from the 30%/60% interface, diluted with fresh buffer, and centrifuged (95000*g*, 0 °C, 60 min), and the pellet was resuspended in 5 mL of buffer. This suspension was dialyzed overnight in 1 L of buffer containing 10 g of Amberlite XAD-2 and was aliquoted, frozen in liquid nitrogen, and stored at −20 °C.

Lipid substitutions were carried out according to the method of Johannsson et al. (1981). Lipids (1.3 μmol) were sonicated briefly with 0.5 mg of cholate in 50 μL of buffer [250 mM sucrose, 1 M KCl, 5 mM MgATP, and 50 mM potassium phosphate (pH 8.0)], and this mixture was incubated with 0.14–0.18 mg of ATPase at 0 °C. (For titrations with DPPC, samples were incubated initially at 42 °C for 10 min.) The time allowed for equilibration was 90 min unless stated otherwise. Two to six microliters of the assay mixture was taken for ATPase assay and fluorescence analysis, the samples being diluted at least 500-fold (final volume for determination of ATPase activity was 2.5 mL and for fluorescence analysis 3 mL). Lipid–ATPase complexes were also prepared by the centrifugation procedure of Warren et al. (1974b).

ATPase activity was measured as outlined by Warren et al. (1974b) except that the buffer was 40 mM Hepes (pH 7.2) and the Ca^{2+} concentration was maintained at the optimal value (pCa^{2+} 6.0) with 1.01 mM EGTA and 0.91 mM $CaCl_2$. Unless otherwise stated, assays were carried out at 37 °C. Fluorescence measurements were made in buffer (40 mM Hepes, 100 mM NaCl, and 1 mM EGTA, pH 7.2) by using either Spex fluorolog or Perkin-Elmer MPF 44A fluorometers. Fluorescence was excited at 285 nm and detected at 340 nm.

Protein was estimated either by the biuret method or using the extinction coefficient given by Thorley-Lawson & Green (1973).

Results

Physical Properties of BRPC. ESR spectra for the spin-labeled probes [12,3]SL and [1,14]SL in BRPC and DOPC at 20 °C are shown in Figure 1. It is clear that both lipids are in the liquid-crystalline phase. For [12,3]SL the order parameter calculated using the method given by Gaffney (1976) is 0.65 in BRPC and 0.58 in DOPC. For [1,14]SL the approximate τ parameter calculated as in Likhtenshtein (1976) is 1.9×10^{-9} s in BRPC and 1.1×10^{-9} s in DOPC. These data suggested that the fluidity for the spin-labels in BRPC is somewhat less than in DOPC.

In a number of experiments, McConnell and co-workers (McConnell, 1976) have shown that changes in the distribution of the spin-label Tempo between aqueous and lipid phases can be used to detect phase changes in lipid bilayers, since the partitioning of Tempo into lipids in the liquid-crystalline phase is considerably greater than into the same lipids in the gel phase. The partition can be defined by the parameter f given by

$$f = B/(B + F) \quad (1)$$

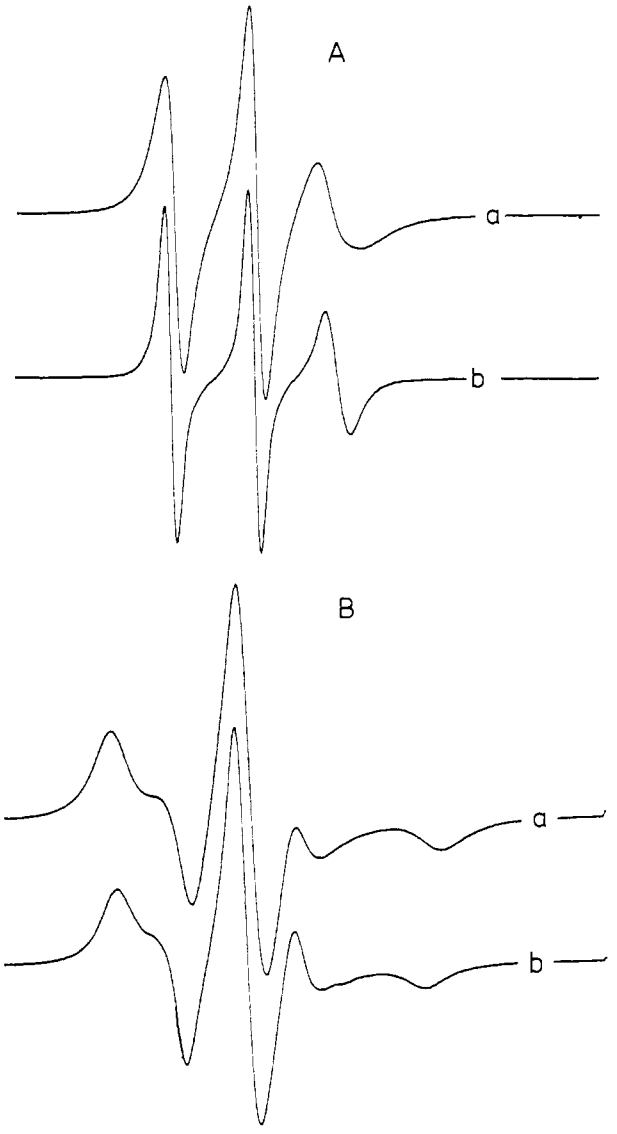

FIGURE 1: ESR spectra at 20 °C of (A) [1,14]SL and (B) [12,3]SL in bilayers of (a) BRPC and (b) DOPC.

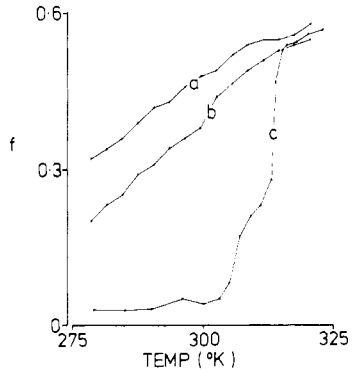

FIGURE 2: Effect of temperature on the partition parameter f of Tempo for liposomes of (a) DOPC, (b) BRPC, and (c) DPPC.

where B is the amplitude of the ESR signal due to lipid bound probe and F is the amplitude of the ESR signal due to the probe in the aqueous phase.

Figure 2 shows the variation of the partition parameter f for DPPC, DOPC, and BRPC. For DPPC, breaks in the plot of f against T can be seen at 314 K and about 303 K which correspond to the temperatures of the liquid-crystalline to gel transition. There are no obvious break points in the data shown

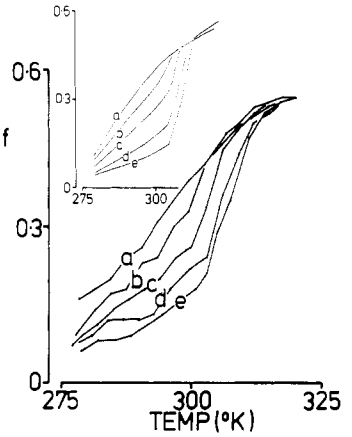

FIGURE 3: Effect of temperature on the partition parameter f of Tempo into mixtures of DPPC–BRPC. The proportion of DPPC in the mixture was (a) 20%, (b) 40%, (c) 60%, (d) 80%, and (e) 90%. (Inset) Simulated temperature–partition parameter f curves of above DPPC–BRPC mixtures calculated from the phase diagram shown in Figure 4.

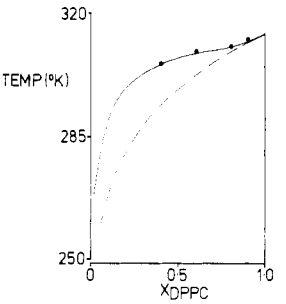

FIGURE 4: Phase diagram for mixtures of DPPC with BRPC. The solid line shows the best fit to the experimental data using the model outlined (eq 3), assuming nonideal mixing of lipids in the liquid-crystalline phase and total immiscibility in the gel phase. The broken line shows the theoretical curve assuming ideal mixing in the liquid-crystalline phase and total immiscibility in the gel phase (eq 2). The points represent upper break point temperatures taken from the plots shown in Figure 3 for high mole fractions of DPPC. The phase diagram for mixtures containing a low mole fraction of DPPC is confirmed by simulation of Tempo plots (Figure 3, inset). The phase diagram for mixtures of DPPC with DOPC is identical with that shown.

for DOPC and BRPC (Figure 2). For DOPC the reported liquid-crystalline to gel transition is −22 °C (Phillips et al., 1970), and from the data in Figure 2, the phase transition temperature for BRPC would seem to be below 5 °C, the lowest temperature examined. This is consistent with the melting points of the constituent fatty acids. All the common phosphatidylcholines exhibit phase transition temperatures lower than the melting temperatures of the corresponding fatty acids [see Lee (1977)]. Thus the phase transition temperature of −22 °C for DOPC can be compared with +16 °C for oleic acid. We have determined the melting point of dibromooleic acid as 25 °C, suggesting that the phase transition temperature could be below 0 °C. Attempts to determine the transition temperature for BRPC by differential scanning calorimetry were unsuccessful; the lipid endotherm appears beneath the large peak due to the freezing of water. This would put the BRPC phase transition in the range of about −7 to +7 °C. The data in Figure 2 also show that the solubility of Tempo in BRPC is somewhat less than in DOPC, again suggesting that the brominated lipid gives a slightly less fluid bilayer.

As shown by McConnell (1976) it is also possible to use Tempo solubility data to generate phase diagrams for mixtures of lipids. Data for mixtures of DPPC with BRPC are given

in Figure 3. For mixtures with a mole fraction of DPPC down to 0.4, it is possible to detect an upper break point in these plots, and these are plotted in Figure 4. A lower break point is not detected in the experimentally accessible temperature range, suggesting that BRPC is largely immiscible with DPPC in the gel phase.

If BRPC and DOPC are immiscible with DPPC in the gel phase, but mix ideally in the liquid-crystalline phase, then a phase diagram can be readily generated from the equation (Lee, 1978)

$$\ln x_{DPPC}^{L} = \frac{\Delta H_{DPPC}}{R}\left(\frac{1}{T_{DPPC}} - \frac{1}{T}\right) \quad (2)$$

where R is the gas constant, T_{DPPC} and ΔH_{DPPC} are the phase transition temperature and enthalpy change for DPPC, respectively, and x_{DPPC}^{L} is the mole fraction of DPPC in the liquid-crystalline phase at temperature T. A similar equation can be written for the freezing curve of BRPC but is irrelevant here as it will not appear in the temperature range employed. Taking the transition enthalpy for DPPC to be 8500 cal/mol (Wilkinson & Nagle, 1981), the calculated phase diagram is given by the broken line in Figure 4 and clearly disagrees with the experimental data. Such disagreement has been observed for a wide variety of other lipid mixtures and attributed to a nonideal mixing of lipids in the liquid-crystalline phase (Lee, 1978). Such nonideality can be described in terms of a nonideality parameter, ρ_0, where the temperature T at which the mixture of mole fraction x_{DPPC}^{L} exists in the liquid-crystalline phase is related to the temperature T^{ideal} at which the transition would have occurred had the mixing been ideal by (Lee, 1978)

$$T = T^{ideal}\left[1 + \frac{\rho_0(1 - x_{DPPC}^{L})^2}{\Delta H_{DPPC}}\right] \quad (3)$$

As shown in Figure 4, a good fit to the experimental points can be obtained with $\rho_0 = 900$ cal/mol. An identical phase diagram is obtained for mixtures of DPPC with DOPC.

To better define the phase diagram experimentally, it is necessary to obtain data at lower mole fractions of DPPC, but as shown in Figure 3 no clear break points can be observed in the ESR data for such mixtures. This problem can be overcome by using the phase diagram of Figure 4 to generate theoretical Tempo solubility plots which can then be compared to the experimental data. The procedure has been described in detail by Shimshick & McConnell (1973). Calculated f values obtained from the phase diagram of Figure 4 are shown in Figure 3 (inset). Agreement with the experimental data is good at lower mole fractions of DPPC and confirms the major features of the phase diagram. As found by Shimshick & McConnell (1973) the calculated data for higher molar ratios of DPPC, however, shows too low a solubility for Tempo in the gel phase. This can probably be attributed to a mismatch of packing between the gel and liquid-crystalline phases, resulting in increased disorder in the gel phase and increased solubility for Tempo.

The observation that the same values of the nonideality parameter ρ_0 describe the mixing of DPPC with both DOPC and BRPC confirms the similarity of the latter two lipids.

Effects of BRPC on Enzyme Activity. When the lipid substitution technique of Warren et al. (1974a) is used, it is possible to replace the original lipids around the $(Ca^{2+}$–$Mg^{2+})$-ATPase with exogenous phospholipids. The final enzyme activity of the preparation depends on the structure of the added phospholipid. Substitution of the original lipids by BRPC leads to an increase in activity from 14 to 16 IU. With DOPC the activity increases to 20 IU with the same time course. The slightly lower activity for the ATPase substituted with BRPC than with DOPC would reflect the slightly lower "fluidity" of BRPC detected by ESR. It is clear that BRPC is capable of supporting full activity of the ATPase in these preparations and is behaving as a typical phospholipid.

Table I: Relative Binding Constants for the Binding of Exogenous Lipids to $(Ca^{2+}$–$Mg^{2+})$-ATPase (Expressed Relative to DOPC) and the Fluorescence of Substituted ATPase Relative to Native $(Ca^{2+}$–$Mg^{2+})$-ATPase

lipid	$K_{A/DOPC}$	rel fluorescence
DMPC	0.83	1.17
DPPC (45 °C)	0.83	
DPPC (37 °C)	0.53	1.23
DPPC (10 °C)	0.04	
brain PS	1.0	1.10
brain PS + Ca^{2+}	0.45	
egg PE	0.42	1.01
DOPC		1.19

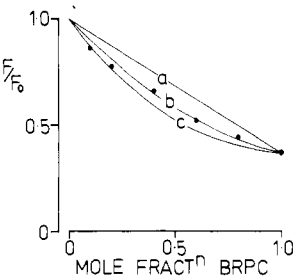

FIGURE 5: Effect of increasing the mole fraction of BRPC in BRPC–DOPC mixtures on the relative intensity (F/F_0) of tryptophan fluorescence of $(Ca^{2+}$–$Mg^{2+})$-ATPase at 37 °C. The curves shown are theoretical profiles for quenching, assuming the model in eq 4 with (a) $n = 1$, (b) $n = 1.6$, and (c) $n = 2$.

BRPC as a Fluorescence Quencher. The $(Ca^{2+}$–$Mg^{2+})$-ATPase contains a large number of tryptophan residues in hydrophobic regions of the protein structure (Allen et al., 1980) whose fluorescence can be quenched by hydrophobic compounds (Moules et al., 1982). As shown in Table I, protein fluorescence depends on the nature of the surrounding lipid, at least for lipid–protein complexes prepared by the lipid substitution technique employed here. Fluorescence was higher with the phosphatidycholines than with phosphatidylserine or phosphatidylethanolamine. Replacement of the original lipid with BRPC, however, led to a decrease in fluorescence, to about 38% of that seen with DOPC. This decrease in fluorescence was complete within about 5 min, a time course which matched the change in ATPase activity caused by BRPC. If cholate (which facilitates the exchange of lipid) was omitted from the substitution procedure, then neither the fluorescence nor the activity of the ATPase was affected by the addition of BRPC or DOPC.

When the centrifugation procedure of Warren et al. (1974b) is used, substituted lipid–ATPase complexes can be prepared with a 30:1 lipid:protein ratio. These complexes show full ATPase activity. Complexes prepared in this way with BRPC also show a fluorescence 38% of those prepared with DOPC.

When the ATPase was reconstituted with mixtures of BRPC and DOPC, the observed fluorescence quenching depended on the mole fraction of BRPC in the mixture (Figure 5). A similar observation was made by London & Feigenson (1981a) using spin-labeled phospholipid as quenching agent. Because of the short fluorescence decay time for tryptophan, quenching in these systems would be expected to be largely static. Support for static quenching also comes from Figure 6 which

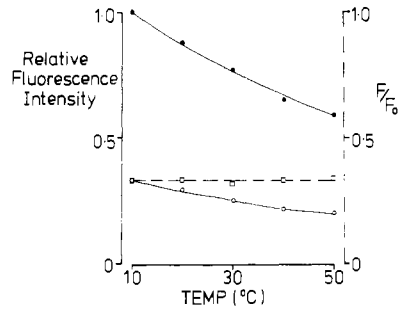

FIGURE 6: Effect of temperature on the intensity of tryptophan fluorescence for DOPC–ATPase (●) and BRPC–ATPase (○). The broken line shows the data expressed as F/F_0.

shows that temperature has no effect on the fluorescence quenching (F/F_0) by BRPC alone. As discussed by London & Feigenson (1981a), static quenching means that fluorescence is quenched only by annular lipid, and if BRPC and DOPC form an ideal mixture, then the fluorescence intensity F is related to the mole fraction of BRPC in the mixture x_{BRPC} by

$$F/F_0 = (F_0 - F_{min})(1 - x_{BRPC})^n + F_{min} \quad (4)$$

where F_0 is the fluorescence of the ATPase in DOPC alone, F_{min} is that in BRPC alone, and n is the number of lipid sites around an average tryptophan residue. This analysis assumes that there is a subset of completely nonquenchable tryptophan residues, presumably buried within the center of the protein. This subset accounts for the residual fluorescence seen in the presence of BRPC alone. The analysis is probably an oversimplification, but nevertheless the equation describes the experimental data well with $n = 1.6$ (Figure 5). Since BRPC contains two fatty acyl chains containing quenching bromine atoms, this would correspond to about three fatty acyl chains being within quenching distance of each quenchable tryptophan residue. Using a spin-labeled phospholipid containing one spin-labeled fatty acyl chain, London & Feigenson (1981a) found a value of $n = 2$.

More interestingly it is possible to use fluorescence quenching data to obtain relative binding constants for lipids to the ATPase (London & Feigenson, 1981b). A relative binding constant can be defined as

$$K_{A/B} = K_A/K_B \quad (5)$$

where K_A and K_B are intrinsic binding constants for lipids A and B, respectively, to the ATPase. Fluorescence quenching plots provide a measure of the relative ability of a lipid under study to displace BRPC from around the ATPase compared to DOPC. The binding constant for lipid A relative to DOPC, $K_{A/DOPC}$, is given by

$$K_{A/DOPC} = \frac{x_A(1 - x_{DOPC})}{(1 - x_A)x_{DOPC}} \quad (6)$$

where x_A and x_{DOPC} are the mole fractions of lipid A and DOPC, respectively, which give the same level of fluorescence quenching in mixtures with BRPC.

For mixtures of BRPC with DMPC, brain phosphatidylserine or DPPC in the liquid-crystalline phase at 45 °C, fluorescence quenching is rather similar to that for mixtures with DOPC (Figure 7A–C). For mixtures with DPPC at lower temperatures, with brain phosphatidylserine in the presence of Ca^{2+} or with phosphatidylethanolamine from egg yolk (Figure 7A–C), however, the extent of fluorescence quenching is greater for a given mole fraction of nonquenching lipid than for mixtures with DOPC as the nonquenching lipid

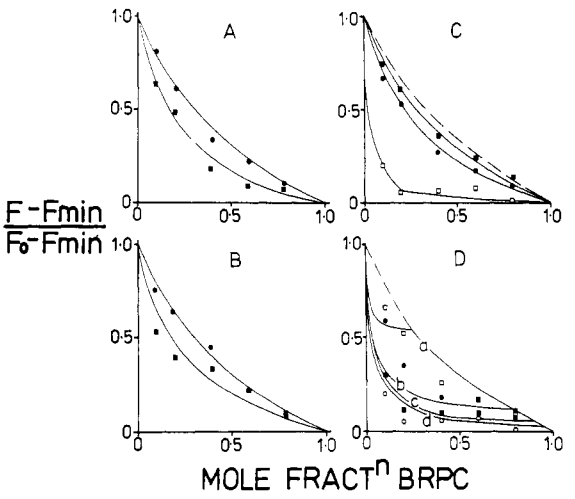

FIGURE 7: Relative quenching of $(Ca^{2+}–Mg^{2+})$-ATPase fluorescence $[(F - F_{min})/(F_0 - F_{min})]$ by BRPC in the following: (A) mixture with DMPC (●) and egg PE (■); (B) mixtures with brain PS in the absence of (●) and presence of 10 mM Ca^{2+} (■); (C) mixtures with DPPC at 45 (■), 37 (●), and 10 °C (□). The broken line shows the fluorescence quenching profile for BRPC–DOPC mixtures at 37 °C. In (D) a simulation of the quenching of $(Ca^{2+}–Mg^{2+})$-ATPase fluorescence in BRPC–DPPC mixtures at (a) 37, (b) 30, (c) 20, and (d) 10 °C is outlined. The corresponding experimental data are also shown: 37 (□), 30 (●), 20 (■), and 10 °C (○). The broken line shows the quenching profile for BRPC–DPPC at 45 °C when all the DPPC is in the liquid-crystalline phase.

(corresponding to weaker binding to the ATPase). Table I lists the values of relative binding constants obtained using eq 6.

The relative binding constants given in Table I show that any selectivity of the ATPase for lipid is small, except for DPPC at low temperatures. Since DPPC at low temperatures will be in the gel phase, it is likely that this selectivity reflects a relative preference of the ATPase for lipid in the liquid-crystalline phase over that in the gel phase. The fluorescence quenching data for mixtures of DPPC and DOPC given in Figure 7C should therefore be explainable in terms of the phase diagram shown in Figure 4. This kind of problem has been analyzed by London & Feigenson (1981c) in a study of fluorescence quenching of diphenylhexatriene in mixtures of lipids. It is assumed that the distribution of ATPase between liquid-crystalline and gel phase lipid can be described by a distribution constant K:

$$K = \frac{[ATPase]_L[lipid]_G}{[ATPase]_G[lipid]_L} \quad (7)$$

where $[ATPase]_L$ and $[ATPase]_G$ are the fraction of ATPase in the liquid-crystalline and gel phases, respectively, and $[lipid]_L$ and $[lipid]_G$ are the fractions of lipid in the two phases. The extent of fluorescence quenching is then given by

$$F'_{obsd} = [ATPase]_L F'_L + [ATPase]_G F'_G \quad (8)$$

where F' is the relative fluorescence quenching:

$$F' = \frac{F - F_{min}}{F_0 - F_{min}} \quad (9)$$

and the subscripts refer to the total observed quenching and to that in the liquid-crystalline and gel phases, respectively. From the phase diagram we can read off the mole fraction of BRPC in the liquid-crystalline phase for any given mixture and temperature. Then from the fluorescence quenching curve for mixtures of DPPC–BRPC at 45 °C (when all the lipid is in the liquid-crystalline phase; Figure 7C) we can determine the fluoresence quenching F'_L for a mixture with this mole

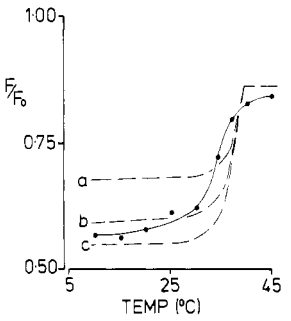

FIGURE 8: Effect of temperature on the quenching of $(Ca^{2+}-Mg^{2+})$-ATPase in mixtures of 10% BRPC–90% DPPC. The broken lines are simulated curves for these data using the model given by eq 10, assuming values for K of (a) 10, (b) 20, and (c) 30.

fraction of BRPC. Since the gel phase lipid over our temperature range is largely DPPC, F'_G is close to one. To employ eq 7 we also need to know the relative amounts of lipid in the two phases. This is obtained from the phase diagram by using the lever rule [see Lee (1977)] as

$$\frac{[\text{lipid}]_G}{[\text{lipid}]_L} = \frac{x_{\text{BRPC}}{}^L - x_{\text{BRPC}}}{x_{\text{BRPC}} - x_{\text{BRPC}}{}^G} \tag{10}$$

where x_{BRPC} is the total mole fraction of BRPC in the mixture and $x_{\text{BRPC}}{}^L$ and $x_{\text{BRPC}}{}^G$ are the mole fractions in the liquid-crystalline and gel phases, respectively. In our case, $x_{\text{BRPC}}{}^G = 0$. These equations can now be combined to derive fluorescence quenching curves as a function of temperature for particular values of the distribution constant K. The value of K which gives the best fit to the experimental data is 30 (Figure 7D) which is similar to the relative binding constant $K_{A/DOPC}$ for DPPC at 10 °C (Table I). This is expected since at 10 °C almost all of the DPPC will be in the gel phase, and thus $K_{A/DOPC}$ will be a measure of the relative affinity of ATPase for lipids in the gel and liquid-crystalline phases. At higher temperatures more of the DPPC will be in the liquid-crystalline phase, and hence $K_{A/DOPC}$ will no longer simply reflect partitioning between the two phases.

The same approach can be used to fit data for fluorescence quenching in mixtures of BRPC and DPPC as a function of temperature. Figure 8 shows the observed quenching in a mixture of 90% DPPC and 10% BRPC. With increasing temperature there is an increase in fluorescence, with the major change being centered at about 35 °C. The figure also shows three curves simulated with $K = 10$, 20, and 30. Again it is clear that best agreement is obtained with $K = 30$. The major disagreement between the theoretical and experimental curves is that the "transition region" of the experimental curve appears about 2 °C below that of the theoretical curve. In the theoretical calculations any possible effects of the ATPase molecules on the phase transition properties of the lipids have been ignored, and this is obviously an oversimplification. Measurements of enzyme activity for the ATPase in the presence of DPPC (Warren et al., 1974a) and spin-label measurements for the same system (Hesketh et al., 1976) show that for lipid around the ATPase, the transition between fluid and solid phases occurs at a somewhat lower temperature and over a wider range of temperatures than for DPPC alone. In activity plots, for example, breaks are seen at 28 and 38 °C (Warren et al., 1974a). An effect of protein on the transition of annular DPPC would similarly explain the higher than expected fluorescence seen at higher molar ratios of DPPC at 30 °C in DPPC–BRPC mixtures (Figure 7D).

Effects of Lipids on ATPase Activity. Figure 9 shows how ATPase activity at 37 °C varies with lipid composition in

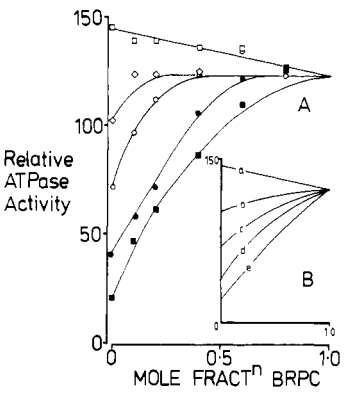

FIGURE 9: (A) Effect on ATPase activity of reconstituting $(Ca^{2+}-Mg^{2+})$-ATPase with various mole fractions of BRPC plus DOPC (□), brain PS (○), egg PE (◇), DPPC (●), and DMPC (■). Activities are measured at 37 °C and expressed relative to that of the original unsubstituted $(Ca^{2+}-Mg^{2+})$-ATPase. (B) Simulated activity profiles for the above data using the model given by eq 12: (a) DOPC, (b) egg PE, (c) brain PS, (d) DPPC, and (e) DMPC.

mixtures with BRPC. It is clear that ATPase activity is very sensitive to the nature of the surrounding lipid: values for activities in the pure lipids plotted in Figure 9 agree with those reported previously (Bennett et al., 1978; Warren et al., 1974a). It is possible to use the relative binding constants to calculate ATPase activity in lipid mixtures using a simple model. The relative binding constant $K_{A/B}$ gives the distribution of lipids A and B in the annulus around the protein as

$$K_{A/B} = \frac{[A][BP]}{[B][AP]} \tag{11}$$

where [A] and [B] are the fractions of the two lipids in the mixture and [AP] and [BP] are the fractions of ATPase bound to A and B, respectively. This equation takes account of the fact that since only ca. 30 lipid molecules are bound per ATPase molecule, the lipid pool present in the mixtures used is not significantly depleted by binding to protein. If the activity of the ATPase in a mixture of two lipids is equal to a weighted sum of the activities of those in the two separated lipids, then

$$[\text{activity}]^{\text{obsd}} = [AP][\text{activity}]^A + [BP][\text{activity}]^B \tag{12}$$

where the superscripts refer to activities in the final mixture and in pure lipids A and B, respectively.

In the fluorescence experiments the relative lipid binding constants $K_{A/B}$ refer to binding relative to DOPC. As described above, we expect the binding constant for ATPase to BRPC to be very similar to that for DOPC, so that the $K_{A/B}$ values should also represent lipid binding relative to BRPC. Making this assumption we can then use the values from Table I in the above calculations. The theoretically calculated activity profiles are shown in Figure 9B. Although the similarity between the experimental and theoretical curves is reasonable, the data are not of course sensitive enough to validate the model and simply show that the simple model is, at present, sufficient.

Discussion

Brominated phospholipids are readily prepared from phospholipids containing unsaturated fatty acyl chains. Addition of two bulky bromine atoms across a C–C cis double bond results in a fatty acyl chain whose packing properties are more like the original unsaturated chain than they are like the corresponding fully saturated chain. Thus we show that the brominated phospholipid (BRPC) obtain by bromination of dioleoylphosphatidylcholine has a gel to liquid-crystalline

phase transition below 5 °C and, as detected by ESR probes, is in a state of fluidity, at ambient temperatures, comparable to dioleoylphosphatidylcholine.

The brominated phospholipid quenches the fluorescence of the (Ca^{2+}–Mg^{2+})-ATPase by a static mechanism and so can be used to assess the ability of phospholipids to enter the annulus around the phospholipid. Fluorescence quenching has been used previously to study lipid selectivity, employing a spin-labeled phospholipid as quencher (London & Feigenson, 1981a,b). The disadvantage of the spin-label is its polarity, which significantly alters the properties of fatty acyl chains (Cadenhead et al., 1975). This might be reflected in the low activity (2 IU) observed for the (Ca^{2+}–Mg^{2+})-ATPase reconstituted with spin-labeled phospholipid (London & Feigenson, 1981b) which can be compared to values of 20 and 16 IU that we find for reconstitution with DOPC and the brominated analogue BRPC, respectively.

The lipid binding constants relative to DOPC that we obtain are listed in Table I. Comparison of the relative values for DMPC and DPPC in the liquid-crystalline state show that there is little selectivity on the basis of fatty acyl chain length. This confirms the observations of London & Feigenson (1981b). Interestingly, however, the ATPase activities supported by both DMPC and DPPC are considerably less than those supported by DOPC. The chain-length dependence of ATPase activity has been attributed by both Caffrey & Feigenson (1981) and Johannsson et al. (1981) to the existence of an optimal membrane thickness for the ATPase. If the fatty acyl chains are either too long or too short, interaction with the hydrophobic surface of the ATPase is suboptimal, leading to conformational changes in the ATPase and thus to loss of activity. The difference in free energy of binding of two lipids to the surface of the ATPase is related to the relative binding constants of the two lipids by

$$\Delta G^\circ_A - \Delta G^\circ_B = -RT \ln K_{A/B} \qquad (13)$$

Since the relative binding constants for DMPC, DPPC, and DOPC are close to unity, the free energies of binding of these lipids must be very similar. In general the strength of binding of long-chain amphiphiles to hydrophobic sites increases markedly with increasing chain length (Tanford, 1980). Since a bilayer of DMPC is thinner than one of DOPC, it would be expected to have a smaller hydrophobic interaction energy with the surface of the ATPase, leading to a reduction in binding energy. This is not observed. One possible explanation could be that the bilayer distorts near the ATPase to form a dimple to maintain the optimal bilayer thickness in the annulus, but calculations by Caffrey & Feigenson (1981) suggest that this may be energetically too unfavorable. An alternative possibility might be that in bilayers of suboptimal thickness the ATPase distorts in such a way that its hydrophobic surface still matches the thickness of the bilayer, with increased hydrophobic interactions within the polypeptide chain making up for lost hydrophobic interactions with the fatty acyl chains. Such a distortion could well lead to large changes in ATPase activity.

Interactions of phospholipids with the ATPase also seem to be relatively insensitive to the lipid head group. The relative binding constant for the negatively charged phosphatidylserine is unity in the the absence of calcium. The smaller binding constant for egg phosphatidylethanolamine could well be due to the differences in phase behavior reported for phosphatidylcholines and phosphatidylethanolamines: Mantsch et al. (1981) have reported that egg phosphatidylethanolamine is in the hexagonal phase at temperatures above 28 °C. Similarly, whereas phosphatidylserines in the absence of Ca^{2+} form bilayers, in the presence of Ca^{2+} a more complex structure is formed (Cullis & de Kruijff, 1979). The affinity of the ATPase for phosphatidylserine in the presence of Ca^{2+} is similar to that for phosphatidylethanolamine.

The most marked effect of lipid phase is exhibited by the temperature dependence of the relative binding constants for DPPC. It is clear that the relative affinity of the ATPase for DPPC in the gel phase is much less than that in the liquid-crystalline phase (Table I). The discrimination we observe between gel and liquid-crystalline phases is significantly greater than that reported by London & Feigenson (1981b) and can be described by a distribution coefficient K of 30 favoring the fluid phase. This is consistent with the freeze–fracture studies of Kleeman & McConnell (1976) which show that in mixtures containing both fluid and solid lipid, the ATPase is highly concentrated in the patches of fluid lipid.

Activities of the ATPase in mixtures of lipid are not related in a simple linear fashion to the mole fractions of the lipids in the mixture (Figure 9). This is the expected result if the ATPase shows differential selectivity for lipids. If it is assumed that the activity of the ATPase is, however, related in a linear fashion to the mole fraction of the lipids in the annulus around it, then the relative binding constants obtained from the fluorescence data can be used to generate activity plots in reasonable agreement with the experimental data (Figure 9). The data obtained here are in broad agreement with the suggestion of Hesketh et al. (1976) that the activity of the ATPase is largely controlled by the nature of the annular lipid, with the bulk lipid having relatively little effect. A comment should be made here on the concept of annular lipid. It has been suggested that this concept only has biological meaning if lipid molecules remain next to the protein for a time comparable to the turnover time of the enzyme (Seelig & Seelig, 1978; Hoffmann et al., 1980). Since the turnover time for (Ca^{2+}–Mg^{2+})-ATPase is of the order of seconds, this would mean that a particular lipid would have to remain in the annulus for a second or so to be important. Deuterium NMR studies show that annular and nonannular lipids exchange at a rate faster than 10^{-3} s (Rice et al., 1979). However, the argument is based on a misunderstanding. It is not the time spent by a particular lipid in the lipid annulus that is important, but whether the time-averaged physical state and chemical composition of the annulus are different from that of bulk lipid. For many of the lipid mixtures studied here the lipid annulus will differ in composition from the bulk lipid (as defined by $K_{A/B}$) on any time scale, despite exchange of lipid between annulus and bulk which is fast on the "biological" time scale.

In our analysis we have assumed that there is no variable aggregation of the ATPase in these systems. It could be that the ATPase is monomeric with an annulus of 30 phospholipid molecules around the monomer, dimeric with an annulus of 60 phospholipids around the dimer, etc. Indeed, there is much evidence that the ATPase is dimeric or tetrameric [see Ikemoto et al. (1981)]. Such aggregation would not affect our analysis. However, a variable oligomerization has been suggested by some workers (Hoffmann et al., 1979) and this would considerably complicate the analysis of our results. On the basis of flash photolysis methods, it has been suggested that the state of oligomerization of the ATPase increases with increasing temperature. We see no evidence for such oligomerization in our fluorescence experiments. On oligomerization, annular lipid will be displaced from the ATPase. In the presence of BRPC such displacement of lipid will lead to a reduction in fluorescence quenching. As shown in Figure 6, this is not observed. It has also been suggested that aggregation of

ATPase molecules with increased protein–protein contact is observed when ATPase is squeezed out of gel phase lipid (Hoffmann et al., 1980). Again any such aggregation would lead to displacement of BRPC and thus to an increase in fluorescence. In mixtures containing 90% DPPC and 10% BRPC this is not observed. The close agreement between theory and experiment for these mixtures (Figures 7D and 8) gives no evidence for protein oligomerization. Finally we note that the fluorescence for BRPC–ATPase complexes are the same at lipid:protein ratios of 30:1 and 800:1, inconsistent with any concentration-dependent protein oligomerization. Studies of the highly protein-enriched purple membrane have shown the presence of protein trimers, separated by regions of phospholipid, with no evidence of oligomerization even at very high protein–lipid molar ratios (Hayward & Stroud, 1981).

Acknowledgments

We thank Jenny Schofield and Elizabeth Burden for preparing the ATPase.

References

Allen, G., Trinnaman, B. J., & Green, N. M. (1980) *Biochem. J. 187*, 591–616.

Ansell, G. B., Hawthorne, J. N., & Dawson, R. M. C. (1973) in *Form and Function of Phospholipids*, Elsevier, Amsterdam.

Bartlett, G. R. (1959) *J. Biol. Chem. 234*, 466–468.

Belcher, R., & Nutten, A. J. (1960) in *Quantitative Inorganic Analysis*, p 216, Butterworths, London.

Bennett, J. P., Smith, G. A., Houslay, M. D., Hesketh, T. R., Metcalfe, J. C., & Warren, G. B. (1978) *Biochim. Biophys. Acta 513*, 310–320.

Berlman, I. B. (1973) *J. Phys. Chem. 77*, 562–567.

Cadenhead, D. A., Kellner, B. M. J., & Muller-Landau, F. (1975) *Biochim. Biophys. Acta 382*, 253–259.

Caffrey, M., & Feigenson, G. W. (1981) *Biochemistry 20*, 1949–1961.

Cullis, P. R., & de Kruijff, B. (1979) *Biochim. Biophys. Acta 559*, 399–420.

Dawidowicz, E. A., & Rothman, J. E. (1976) *Biochim. Biophys. Acta 455*, 621–630.

Gaffney, B. J. (1976) in *Spin Labelling* (Berliner, L. J., Ed.) Academic Press, New York.

Hayward, S. B., & Stroud, R. M. (1981) *J. Mol. Biol. 151*, 491–517.

Hesketh, T. R., Smith, G. A., Houslay, M. D., McGill, K. A., Birdsall, N. J. M., Metcalfe, J. C., & Warren, G. B. (1976) *Biochemistry 15*, 4145–4151.

Hoffmann, W., Sarzala, M. G., & Chapman, D. (1979) *Proc. Natl. Acad. Sci. U.S.A. 76*, 3860–3864.

Hoffmann, W., Sarzala, M. G., Gomez-Fernandez, J. C., Goni, F. M., Restall, C. J., & Chapman, D. (1980) *J. Mol. Biol. 141*, 119–132.

Ikemoto, N., Myao, A., & Karobe, Y. (1981) *J. Biol. Chem. 256*, 10809–10814.

Johannsson, A., Keightley, C. A., Smith, G. A., Richards, C. D., Hesketh, T. R., & Metcalfe, J. C. (1981) *J. Biol. Chem. 256*, 1643–1650.

Kleeman, W., & McConnell, H. M. (1976) *Biochim. Biophys. Acta 419*, 206–222.

Knowles, P. F., Watts, A., & Marsh, D. (1981) *Biochemistry 20*, 5888–5894.

Lee, A. G. (1977) *Biochim. Biophys. Acta 472*, 237–281.

Lee, A. G. (1978) *Biochim. Biophys. Acta 507*, 433–444.

Likhtenshtein, G. I. (1976) in *Spin Labelling Methods in Molecular Biology*, Wiley, New York.

London, E., & Feigenson, G. W. (1981a) *Biochemistry 20*, 1932–1938.

London, E., & Feigenson, G. W. (1981b) *Biochemistry 20*, 1939–1948.

London, E., & Feigenson, G. W. (1981c) *Biochim. Biophys. Acta 649*, 89–97.

Mantsch, H. H., Martin, A., & Cameron, D. G. (1981) *Biochemistry 20*, 3138–3145.

McConnell, H. M. (1976) in *Spin Labelling* (Berliner, L. J., Ed.) Academic Press, New York.

Moore, B. M., Lentz, B. R., Hoechli, M., & Meissner, G. (1981) *Biochemistry 20*, 6810–6817.

Morrison, W. R., & Smith, L. M. (1964) *J. Lipid Res. 5*, 600–608.

Moules, I. K., Rooney, E., & Lee, A. G. (1982) *FEBS Lett. 138*, 95–100.

Parker, C. A. (1968) in *Photoluminescence of Solutions*, Elsevier, Amsterdam.

Phillips, M. C., Ladbrooke, B. D., & Chapman, D. (1970) *Biochim. Biophys. Acta 196*, 35–44.

Rice, D. M., Meadows, M. P., Scheinman, A. O., Goni, F. M., Gomez-Fernandez, J. C., Moscarello, M. A., Chapman, D., & Oldfield, E. (1979) *Biochemistry 18*, 5893–5903.

Sarzala, M. G., Pilarska, M., Zubrycka, E., & Michalak, M. (1975) *Eur. J. Biochem. 57*, 25–34.

Seelig, A., & Seelig, J. (1978) *Hoppe-Seyler's Z. Physiol. Chem. 359*, 1747–1756.

Shimshick, E. J., & McConnell, H. M. (1973) *Biochemistry 12*, 2351–2360.

Tanford, C. (1980) in *The Hydrophobic Effect*, 2nd ed., Wiley, New York.

Thorley-Lawson, D. A., & Green, N. M. (1973) *Eur. J. Biochem. 40*, 403–413.

Warren, G. B., Toon, P. A., Birdsall, N. J. M., Lee, A. G., & Metcalfe, J. C. (1974a) *Biochemistry 13*, 5501–5507.

Warren, G. B., Toon, P. A., Birdsall, N. J. M., Lee, A. G., & Metcalfe, J. C. (1974b) *Proc. Natl. Acad. Sci. U.S.A. 71*, 622–626.

Wilkinson, D. A., & Nagle, J. F. (1981) *Biochemistry 20*, 187–192.